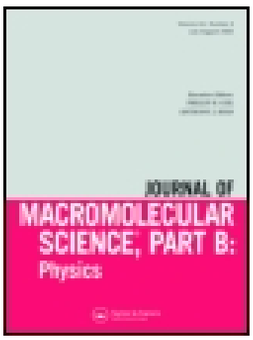

Taylor & Francis
Taylor & Francis Group

Journal of Macromolecular Science, Part B
Physics

ISSN: 0022-2348 (Print) 1525-609X (Online) Journal homepage: http://www.tandfonline.com/loi/lmsb20

Effect of Melanomal Proteins on Sepia Melanin Assembly

Pathomthat Srisuk, Vitor M. Correlo, Isabel B. Leonor, Pasquale Palladino & Rui L. Reis

To cite this article: Pathomthat Srisuk, Vitor M. Correlo, Isabel B. Leonor, Pasquale Palladino & Rui L. Reis (2015): Effect of Melanomal Proteins on Sepia Melanin Assembly, Journal of Macromolecular Science, Part B

To link to this article: http://dx.doi.org/10.1080/00222348.2015.1103430

Accepted online: 06 Oct 2015.

Effect of Melanomal Proteins on Sepia Melanin Assembly

Pathomthat Srisuk[*,†,‡,§], *Vitor M. Correlo*[†,‡], *Isabel B. Leonor*[†,‡], *Pasquale Palladino*[*,†,‡] and *Rui L. Reis*[*,†,‡]

[†]3B's Research Group - University of Minho, Headquarters of the European Institute of Excellence on Tissue Engineering and Regenerative Medicine, AvePark, Zona Industrial da Gandra, S. Cláudio do Barco 4806-909 Caldas das Taipas, Guimarães, Portugal.

[‡]ICVS/3B's - PT Government Associate Laboratory, Braga/Guimarães, Portugal.

[§]Faculty of Pharmaceutical Sciences, Khon Kaen University, 123 Mitraparb Highway, Muang District, Khon Kaen 40002, Thailand.

[*]Corresponding author: Pasquale Palladino: pasquale.palladino@unina.it

[*]Corresponding author: Rui L. Reis: rgreis@dep.uminho.pt (corresponding author)

[a]Corresponding author: Pathomthat Srisuk: pathomthat.srisuk@dep.uminho.pt

[b]Corresponding author: Vitor M. Correlo: vitorcorrelo@dep.uminho.pt

[c]Corresponding author: Isabel B. Leonor: belinha@dep.uminho.pt

Keywords

Sepia melanin self-assembly; amyloid fibrils; cephalopod ink; scanning electron microscopy; Scanning transmission electron microscopy; Atomic force microscopy.

ABSTRACT

Melanins are phenol-based pigments with the potential for widespread applications including bioelectronics and tissue engineering. The concentration-dependent structural transition of sepia melanin in water is analyzed. This biopolymer at high concentration gives the well-known nanospheres, whereas sample dilution gives unforeseen nanofibres exhibiting the structural features of mature amyloid fibrils. We propose a mechanism of pigment self-assembly dependent on the interaction of residual melanosomal protein(s) with eumelanin heteropolymer. Our results contribute to understanding the peculiar physico-chemical properties of this ubiquitous pigment.

INTRODUCTION

Melanin is a pigment useful in nature for photoprotection, radicals scavenging, alarm and camouflage. [1-3] It has been found in most living kingdoms and in fossils like cephalopod ink sacs from the Jurassic period. [4] Sepia ink is the main source of this pigment because it contains large amounts of pure eumelanin, i.e. a heteropolymer, dark and almost insoluble in water, produced starting by oxidation of tyrosine by tyrosinase. [5] The complex morphology changes observed depending on the pigment isolation and preparation methods indicate the need for a better description of the sepia melanin assembly mechanism. [5] Normally, sepia melanin assumes a round shape with nanometric substructures. [6] However, in a few cases, sepia melanin analysis has shown elongated structures for both the natural and synthetic polymers. [6,7] Here we investigate the concentration-dependent structural transition of this biopolymer, mainly by ultrahigh resolution scanning electron microscopy (SEM), of purified melanin from cuttlefish ink (*Sepia officinalis*) finely dispersed in ultra-pure water in a range of concentrations covering several orders of magnitude. We propose a mechanism to explain the observed morphological heterogeneity of this phenol-based pigment, from familiar nanospheres to unforeseen nanofibres, dependent on the well-known presence of interacting melanosomal proteins estimated to be around 6 to 8 % in weight of the water-purified sepia melanin extract. [6,8]

METHODS

Materials

All chemicals were purchased from Sigma-Aldrich (U.S.A.) unless stated otherwise, including the synthetic melanin prepared by oxidation of tyrosine with hydrogen peroxide (purity from thin-layer chromatography (TLC) area 100.0 %; carbon content 54.8 %; nitrogen content 6.9 %). The ink of *Sepia officinalis* (100%) was purchased from the Nortindal Sea Products S. L., Spain.

Isolation and purification

Natural melanin from the ink of *Sepia officinalis* (100 g) was isolated and purified in ultrapure water (200 mL) in a dark vessel. The black slurry ink dispersion was vigorously stirred for 30 min. A pellet was obtained by centrifugation for 15 minutes at 13,000 rpm and 5 °C in a Sigma 2-16K centrifuge (Germany) and the supernatant was removed. The solid was redispersed and this washing procedure was repeated 20 times. The final black pellet was lyophilized and scanning electron microscopy indicated exclusion of contamination with cellular elements. The purified melanin was weighed (1.0 mg/L; 0.100 g/L; 1.00 g/L; 10.0 g/L) and dispersed in ultra-pure water in volumetric flasks. Subsequently, the samples were sonicated for 1 hour at 40 °C. 10 μg/L and 0.10 mg/L samples were obtained by dilution of the 1.0 mg/L suspensions.

SEM and scanning transmission electron microscopy (STEM)

Suspensions were dropped on single-side-polished silicon wafers for SEM, or copper grids coated with a carbon film for STEM, and air-dried in the dark at room temperature. The values of the initial concentrations of the biomaterial dropped on the surfaces are reported below. Samples for SEM were covered with a very thin film (5 nm) of Au-Pd (80-20 weight %) in a

high resolution sputter coater, 208HR Cressington Co. (U.S.A.), coupled to a MTM-20 Cressington High Resolution Thickness Controller. Morphological analysis was conducted by collecting secondary electron (SEM) or transmitted electrons (STEM) images in an Ultra-high resolution Field Emission Gun Scanning Electron Microscope (FEG-SEM), NOVA 200 Nano SEM, FEI Co. (U.S.A.).

Atomic force microscopy (AFM)

Suspensions were dropped on a mica disc (9.9 mm diameter, 0.22-0.27 mm thickness). The observations were performed, scanning the surface for 2 hours and then acquiring the images, in the contact mode at 25 °C using silicon-nitride (Si_3N_4) cantilevers with a spring constant of 0.58 N/m and an E-series piezoceramic scanner (10 mm scanning range) in a Nanoscope III-a Scanning Probe Microscope System (Digital Instruments Inc., U.S.A.).

RESULTS AND DISCUSSION

Sepia melanin assumes the well-known round shape for concentrations between 10.0 g/L to 100 mg/L (Figures 1a, b, c). These nanospheres did not have a homogeneous dimension, ranging between approximately 50 nm and 350 nm, although it has been stated that the dominant constituents of sepia melanin are 150 nm spherical aggregates. [6] In this concentration range the granules of melanin have well-defined contours but, in a few cases (Figure 1a), when the particles were in proximity of each other but not in touch, they appear tethered by thin structures of biomaterial (10 nm x 50 nm). The surface roughness of the granules reflects substructures elsewhere described to be less than 20 nm in diameter. [6] Decreasing the sample concentration to 1.0 mg/L the pigment preserves the spherical shape reported above, but the granules were

mostly connected by and immersed in amorphous biomaterial such that they appeared larger than their true sizes (Figure 1d). Much larger amounts of similar material as that in Fig. 1d has previously been described as melanin disassembled melanin oligomers or residual scaffolding protein(s) released from the interior of the melanin granules during the sonication of the samples. [6] Probably, this glue-like material in Fig. 1d is an extended version of tethering structures observed at higher sample concentrations (Figures 1a, b, c).

Surprisingly, very dilute samples, at 0.1 mg/L and 10 μg/L, showed well defined intertwined fibres with increasing structural complexity and dimensions, starting from a minimum diameter around 11 nm, extending up to several micrometers in length (Figures 2a, b, c and d), and aggregates of spherical and non-spherical particles connected to and emerging from these fibres (Figures 2a, b, d). Other authors have previously shown elongated structures for melanin, defining them as filaments, for the natural polymer, [6] or even fibrils for the synthetic melanin. [7] However, those materials appeared as sticks with a fractal-like assembly in contrast to the twisted morphology observed in our experiments which closely resembles the conformation of mature amyloid fibrils elsewhere reported. [9-13] For full comparison, SEM images at low concentration were also acquired for synthetic melanin, resulting in round-shaped aggregates only without fibril-like structures (Figures 3a and b).

We confidently exclude the possibility of contamination by extrinsic fibres in our samples during handling. If so, these fibrils should be observable at high concentration and within samples of synthetic melanin too, using the same manipulation of samples and same magnification of their images, whereas the fibrils appeared only for natural melanin at low concentration. Moreover, we have observed the nanofibres by two other experimental

techniques, namely atomic force microscopy (AFM) (Figure 4) and scanning transmission electron microscopy (STEM) (Figure 5). The most complex morphology of the fibres was achieved by the SEM sample preparation technique, probably because the surface on which deposited affects the structure and size of the fibril deposits, as recently reported. [14,15] In particular, the silicon wafers used for SEM resulted in particularly fascinating knitting patterns of the filaments showing circular and star-like arrangements (Figure 2), whereas the samples deposited on mica discs (AFM) and copper grids coated with carbon films (STEM) surfaces resulted in branched fibrils only (Figures 4 and 5, respectively).

Unfortunately, the only way that has been reported to separate the eumelanin from associated protein(s) requires harsh conditions that lead to protein(s) and pigment alteration and degradation; it involves long treatment with strong acids at high temperature. [16] Moreover, our attempts to use the typical characterization methods for amyloid were unsuccessful (data not shown) due to the predominant absorbance of eumelanin (more than 92 % in weight of purified sepia melanin) [6,8] in UV, visible and IR ranges of wavelengths. [17,18] Finally, the very low protein amounts in the suspensions where the fibrils appeared (0.1 mg/L and 10 μg/L samples contain 6-8 μg/L and 0.6-0.8 μg/L of protein(s), respectively) is some orders of magnitude lower than that incurred using, for example, circular dichroism, infrared spectroscopy, calorimetry and dye-binding characterization techniques. [19-22]

Although the fibrils formation rate is proportional to the amount of biopolymer, [23] fibrils were predominant only at very low concentrations of our purified samples (Figures 2, 4, and 5). To explain this apparent paradox we propose a mechanism of pigment self-assembly dependent on protein(s)-eumelanin interactions (Figure 6). We suggest that the fibrils and

particles occupy two different energy minima in a complex free energy landscape for sepia melanin folding and assembly. These aggregates are already present before the solvent evaporation, being determined by the starting concentration and treatment of the biomaterial in suspension. The dilution of concentrated suspensions of sepia melanin causes the particles to dissolve and the aggregation of the residual melanosomal protein(s), leading to protein(s)-driven fibrils formation; these would be completely absent in synthetic melanin samples due to absence of the proteins. However, the air-drying of very dilute samples in a relatively short time cannot convert the fibrils into nanoparticles, likely because of the low unfolding rate. On the contrary, the protein(s) fibrillogenesis is impaired by highly concentrated sepia melanin suspensions that favor, instead, the eumelanin-driven pigment aggregation in nanoparticles, in agreement with the inhibition of fibrils formation by polyphenols such as epigallocatechingallate (EGCG). [24,25] In fact, EGCG completely impairs α-synuclein (αS) and amyloid-β (Aβ) fibrils growth and causes the disassembly of preformed micrometric amyloid fibres, trapping and concentrating the αS and Aβ oligomers in spherical aggregates with a diameter ranging between 10 and 100 nm. [24] In this context, it is important to mention that the biosynthesis of the amyloid fibrils and melanin possess an evolutionarily conserved linkage, [26] and, during melanogenesis in vertebrates, eumelanin deposits on the filamentous form of pre-melanosomal glycoprotein (Pmel), similar to Aβ fibrils; this templates and accelerates the formation of pigment. [12,26]. Moreover, it has been suggested that Pmel has a close similarity to melanogenic peroxidase from *Sepia officinalis* because both are components of the melanosomal matrix and are absent from coated vesicles that deliver tyrosinase-related proteins to melanosomes. [27]

CONCLUSIONS

Taken as a whole, the results herein and those of previous studies provide further confidence in our hypothesis of protein-dependent fibrils formation at low concentration of pigment from *Sepia officinalis* and its inhibition by eumelanin particles growth. We believe that these experiments and explanations of the effect of residual melanosomal protein(s) should be beneficial, permitting understanding of the origin of melanins properties and, subsequently, the design of biomimetic materials with applications from physics to medicine. [28-30]

ACKNOWLEDGEMENTS

This work was supported by the European Union's Seventh Framework Programme (FP7/2007-2013) under grant agreement No. REGPOT-CT2012-316331-POLARIS, and by a Khon Kaen University grant to PS.

REFERENCES

1. Ortonne, J.P. Photoprotective properties of skin melanin. Br. J. Dermatol. **2002**, *S61*, 7-10.

2. Herrling, T.; Jung, K.; Fuchs, J. The role of melanin as protector against free radicals in skin and its role as free radical indicator in hair. Spectrochim. Acta A Mol. Biomol. Spectrosc. **2008**, *69*, 1429-1435.

3. Wood, J.B.; Pennoyer, K.E.; Derby, C.D. Ink is a conspecific alarm cue in the Caribbean reef squid, Sepioteuthis sepioidea. J. Exp. Mar. Biol. Ecol. **2008**, *367*, 11-16.

4. Glass, K.; Ito, S.; Wilby, P.R.; Sota, T.; Nakamura, A.; Bowers, C.R.; Vinther, J.; Dutta, S.; Summons, R.; Briggs, D.E.; Wakamatsu, K.; Simon, J.D. Direct chemical evidence for eumelanin pigment from the Jurassic period. Proc. Natl. Acad. Sci. U S A. **2012**, *109*, 10218-10223.

5. Slominski, A.; Tobin, D.J.; Shibahara, S.; Wortsman, J. Melanin pigmentation in mammalian skin and its hormonal regulation. Physiol. Rev. **2004**, *84*, 1155-1228.

6. Liu, Y., Simon, J.D. The effect of preparation procedures on the morphology of melanin from the ink sac of Sepia officinalis. Pigment Cell. Res. **2003**, *16*, 72-80.

7. McQueenie, R.; Sutter, J.; Karolin, J.; Birch, D.J. Eumelanin fibrils. Biomed. Opt. **2012**, *17*, 075001.

8. Sharma, S.; Wagh, S.; Govindarajan, R. Melanosomal proteins role in melanin polymerization. Pigment Cell. Res. **2002**, *15*, 127-133.

9. Sunde, M.; Serpell, L.C.; Bartlam, M.; Fraser, P.E.; Pepys, M.B.; Blake, C.C. Common core structure of amyloid fibrils by synchrotron X-ray diffraction. J. Mol. Biol. **1997**, 273, 729-739.

10. Rochet, J.C.; Lansbury Jr., P.T. Amyloid fibrillogenesis: themes and variations. Curr. Opin. Struct. Biol. **2000**, *10*, 60-68.

11. Jiménez, J.L.; Nettleton, E.J.; Bouchard, M.; Robinson, C.V.; Dobson, C.M.; Saibil, H.R. The protofilament structure of insulin amyloid fibrils. Proc. Natl. Acad. Sci. U S A. **2002**, *99*, 9196-9201.

12. McGlinchey, R.P.; Shewmaker, F.; Hu, K.N.; McPhie, P.; Tycko, R.; Wickner, R.B. Repeat domains of melanosome matrix protein Pmel17 orthologs form amyloid fibrils at the acidic melanosomal pH. J. Biol. Chem. **2011**, *286*, 8385-8393.

13. Adamcik, J.; Mezzenga, R. Proteins Fibrils from a Polymer Physics Perspective. Macromolecules. **2012**, *45*, 1137-1150.

14. Bergkvist, M.; Carlsson, J.; Oscarsson, S. Surface-dependent conformations of human plasma fibronectin adsorbed to silica, mica, and hydrophobic surfaces, studied with use of Atomic Force Microscopy. J. Biomed. Mater. Res. A. **2003**, *64*, 349-356.

15. Moores, B.; Drolle, E.; Attwood, S.J.; Simons, J.; Leonenko, Z. Effect of Surfaces on Amyloid Fibril Formation. PLoS One. **2011**, *6*, e25954.

16. Zeise, L.; Addison, R.B.; Chedekel, M.R. Bio-analytical studies of eumelanins. I. Characterization of melanin the particle. Pigment Cell. Res. **1990**, *3*, 48-53.

17. Panzella, L.; Gentile, G.; D'Errico, G.; Della Vecchia, N.F.; Errico, M.E.; Napolitano, A.; Carfagna, C.; d'Ischia, M. Atypical structural and π-electron features of a melanin polymer that lead to superior free-radical-scavenging properties. Angew. Chem. Int. Ed. Engl. **2013**, *52*, 12684-12687.

18. Centeno, S.A.; Shamir, J. Surface enhanced Raman scattering (SERS) and FTIR characterization of the sepia melanin pigment used in works of art. J. Mol. Struct. **2008**, *873*, 149-159.

19. Khurana, R.; Uversky, V.N.; Nielsen, L.; Fink, A.L. Is Congo red an amyloid-specific dye? J. Biol. Chem. **2001**, *276*, 22715-22721.

20. Nilsson, M.R. Techniques to study amyloid fibril formation in vitro. Methods. **2004**, *34*, 151-160.

21. Hudson, S.A.; Ecroyd, H.; Kee, T.W.; Carver, J.A. The thioflavin T fluorescence assay for amyloid fibril detection can be biased by the presence of exogenous compounds. FEBS J. **2009**, *276*, 5960-5972.

22. Dandurand, J., Samouillan, V.; Lacoste-Ferre, M.H.; Lacabanne, C.; Bochicchio, B.; Pepe, A. Conformational and thermal characterization of a synthetic peptidic fragment inspired from human tropoelastin: Signature of the amyloid fibers. Pathol. Biol. (Paris). **2014**, *62*, 100-107.

23. Morris, A.M.; Watzky, M.A.; Finke, R.G. Protein aggregation kinetics, mechanism, and curve-fitting: a review of the literature. Biochim. Biophys. Acta. **2009**, *1794*, 375-397.

24. Ehrnhoefer, D.E.; Bieschke, J.; Boeddrich, A.; Herbst, M.; Masino, L.; Lurz, R.; Engemann, S.; Pastore, A.; Wanker, E.E. EGCG redirects amyloidogenic polypeptides into unstructured, off-pathway oligomers. Nat. Struct. Mol. Biol. **2008**, *15*, 558-566.

25. Berhanu, W.M.; Masunov, A.E. Atomistic mechanism of polyphenol amyloid aggregation inhibitors: molecular dynamics study of Curcumin, Exifone, and Myricetin interaction with the segment of tau peptide oligomer. J. Biomol. Struct. Dyn. **2015**, *33*, 1399-1411

26. Grimaldi, A.; Girardello, R.; Malagoli, D.; Falabella, P.; Tettamanti, G.; Valvassori, R.; Ottaviani, E.; de Eguileor, M. Amyloid/Melanin distinctive mark in invertebrate immunity. Invertebr. Survival J. **2012**, *9*, 153-162.

27. Palumbo, A.; di Cosmo, A.; Gesualdo, I.; Hearing, V.J. Subcellular localization and function of melanogenic enzymes in the ink gland of Sepia officinalis. Biochem. J. **1997**, *323*, 749-756.

28. Bettinger, C.J.; Bruggeman, J.P.; Misra, A.; Borenstein, J.T.; Langer, R. Biocompatibility of biodegradable semiconducting melanin films for nerve tissue engineering. Biomaterials. **2009**, *30*, 3050-3057.

29. Shanmuganathan, K.; Cho, J.H.; Iyer, P.; Baranowitz, S.; Ellison, C.J. Thermooxidative Stabilization of Polymers Using Natural and Synthetic Melanins. Macromolecules. **2011**, *44*, 9499–9507.

30. Mostert, A.B.; Powell, B.J.; Gentle, I.R.; Meredith, P. On the origin of electrical conductivity in the bio-electronic material melanin. Appl. Phys. Lett. **2012**, *100*, 093701.

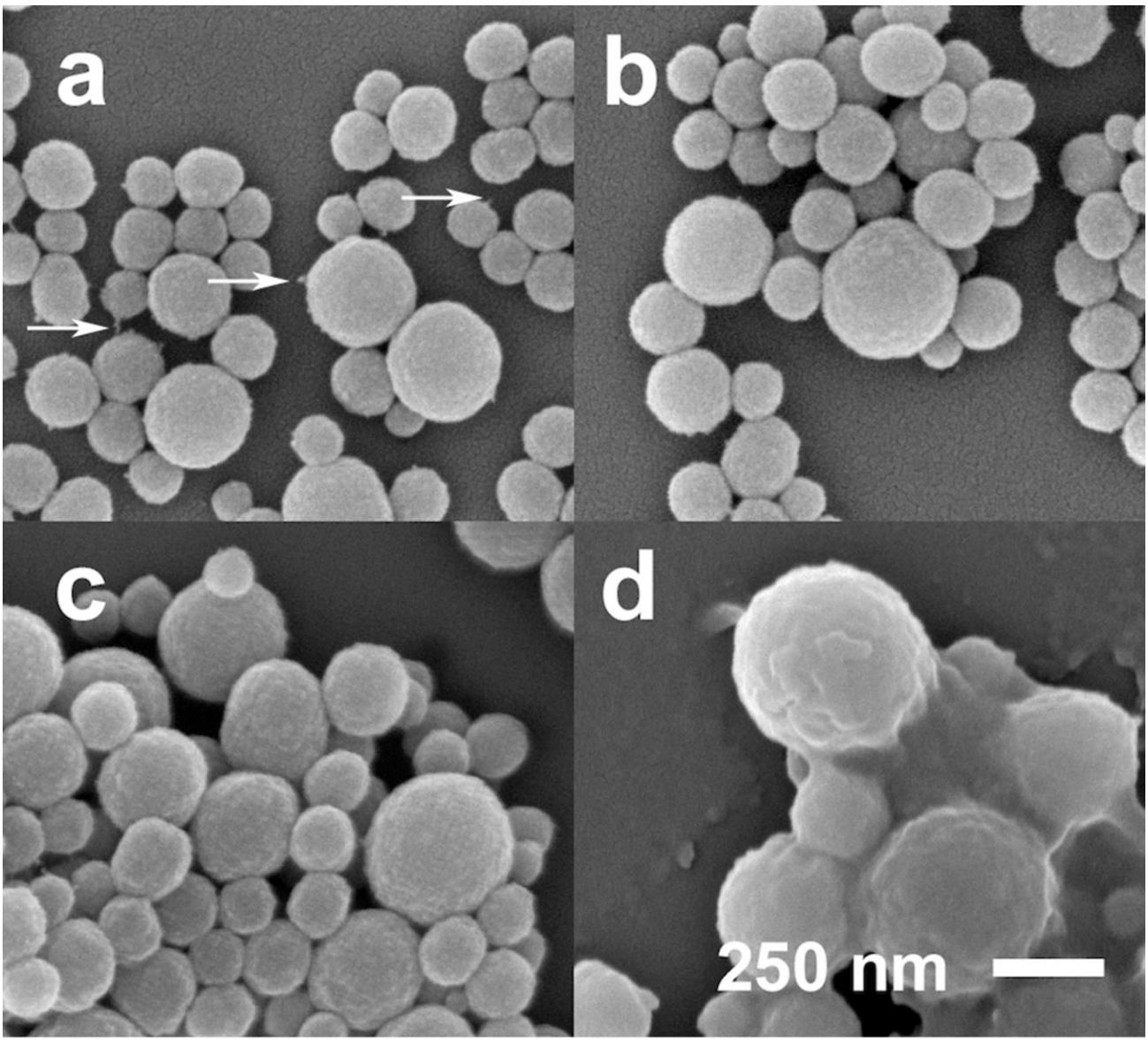

Fig. 1

Figure 1. Morphology of sepia melanin samples air-dried on silicon wafers from water suspensions at 10.0 g/L (a), 1.00 g/L (b), 100 mg/L (c), and 1.0 mg/L (d). Arrows indicate a few projections of smaller size.

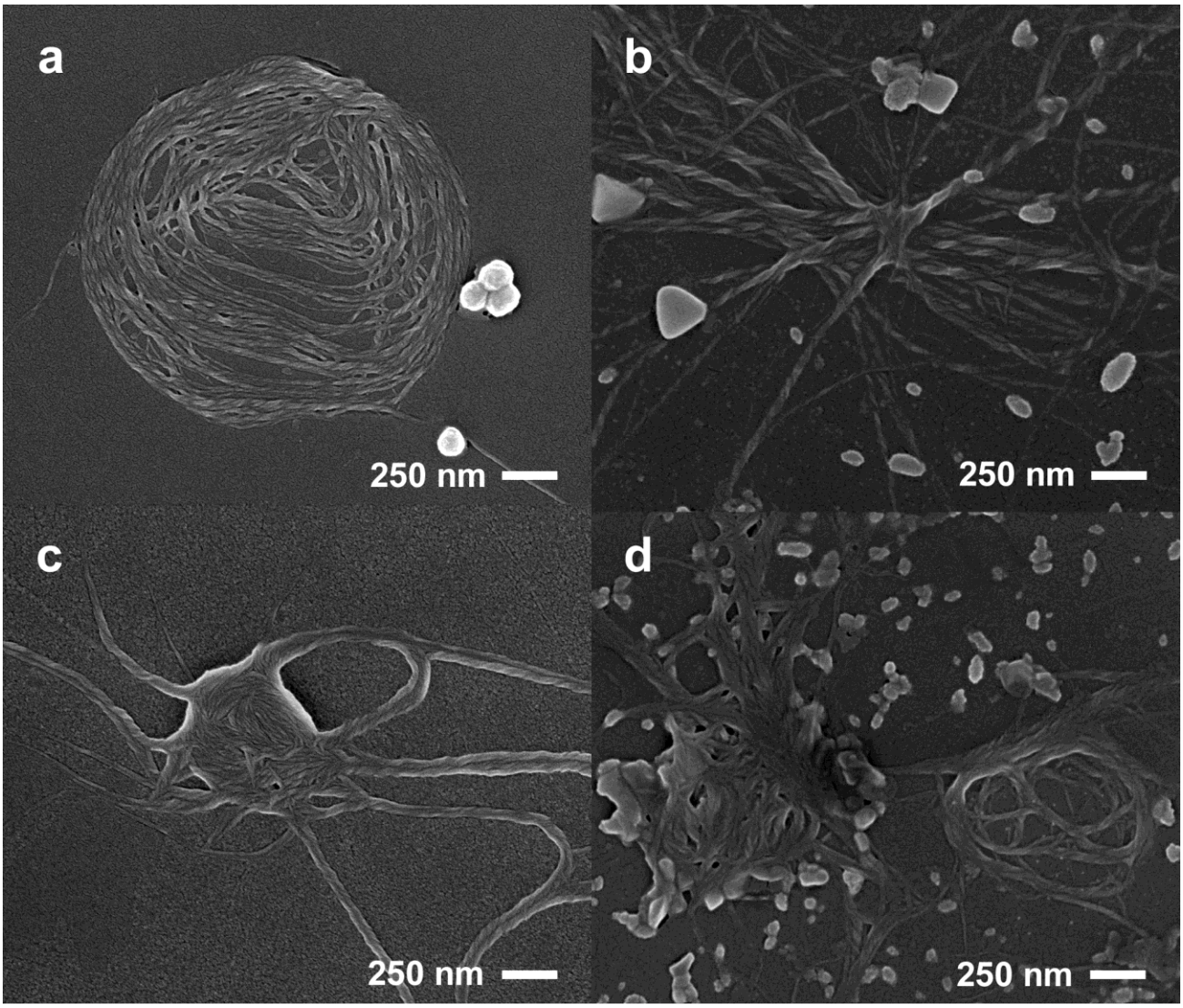

Fig. 2

Figure 2. Morphology of sepia melanin samples air-dried on silicon wafers from water suspensions at 0.10 mg/L (a, b), and 10 μg/L (c, d). Fig. 2a and b, as well as Fig. 2c and d,

represent different regions of the silicon wafers where the SEM images of sepia melanin were acquired.

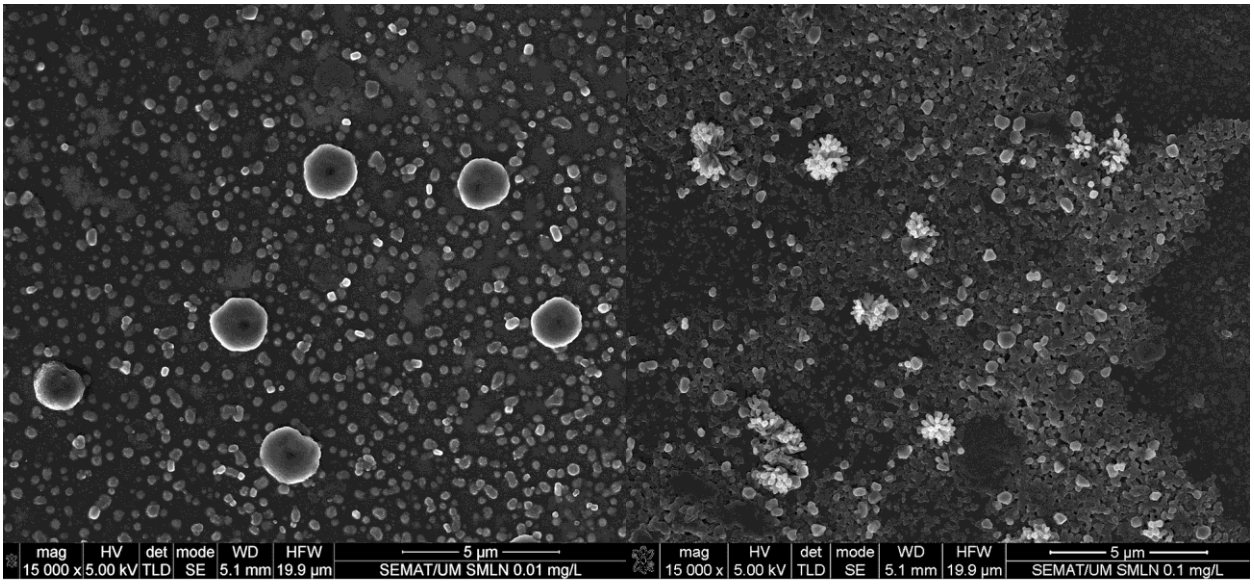

Fig. 3a

Fig. 3b

Figure 3. SEM images of synthetic melanin on silicon wafers from water suspensions at 10 µg/L (a) and 0.10 mg/L (b).

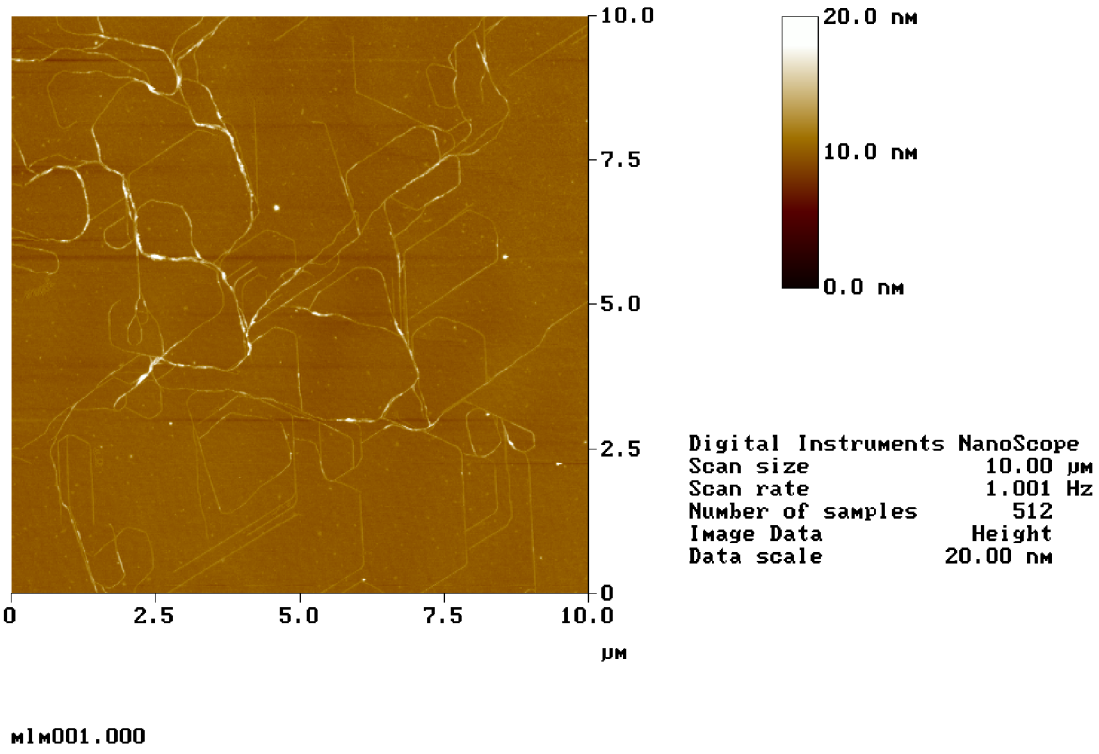

Fig. 4 (color on web

Figure 4. AFM image of sepia melanin sample on a mica disc from water suspensions at 10 µg/L.

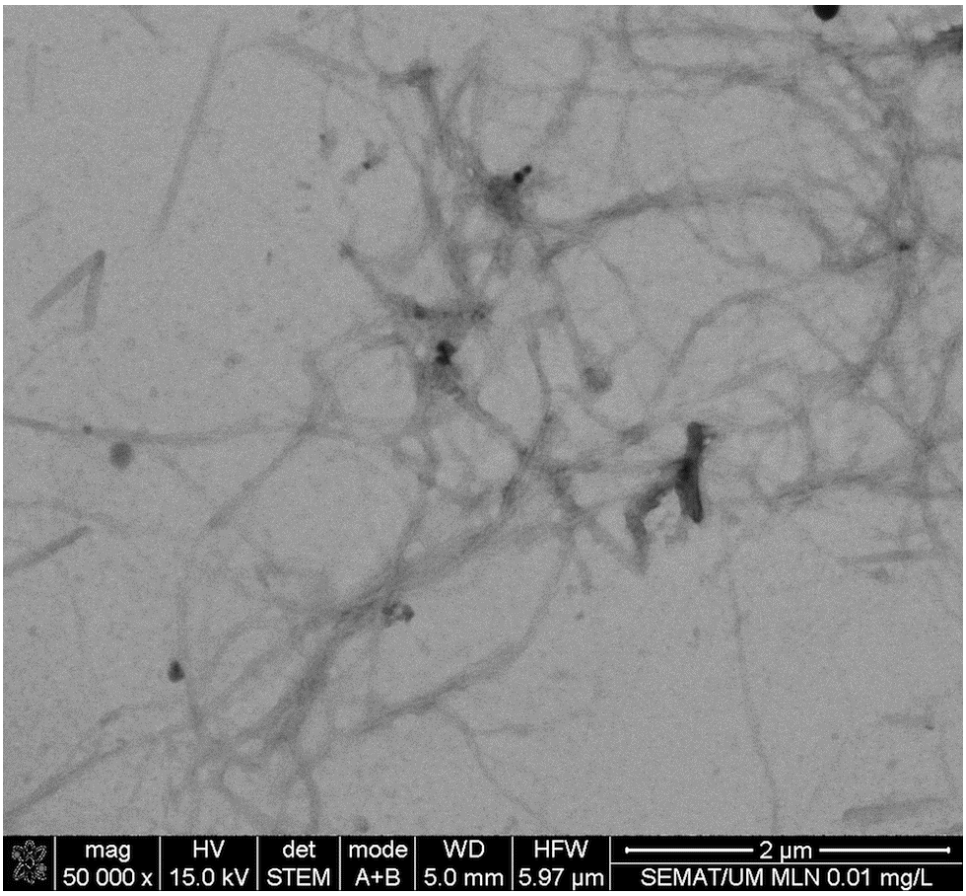

Fig. 5

Figure 5. STEM image of sepia melanin sample air-dried on a copper grid coated with carbon film from water suspensions at 10 µg/L.

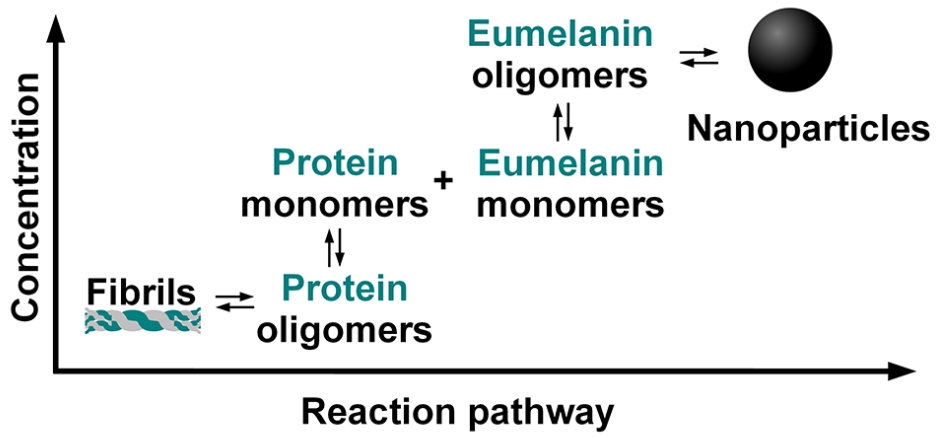

Fig. 6, color on web

Figure 6. Proposed model of eumelanin/protein(s) self-assembly from fibrils to nanoparticles.